NO formation during co-combustion of coal with two thermally treated biomasses

(article starts on next page)

NO formation during co-combustion of coal with two thermally treated biomasses

Thomas Allgurén [a],[*], Klas Andersson [a], Andrew Fry [b], Eric G. Eddings [c]

[a] *Department of Space Earth & Environment, Chalmers University of Technology, Sweden*
[b] *Department of Chemical Engineering, Brigham Young University, Provo, UT, United States of America*
[c] *Department of Chemical Engineering, University of Utah, Salt Lake City, UT, United States of America*

A B S T R A C T

The combustion behavior of biomass as a fuel varies dependent on source of the raw material, but also on the type of pre-treatment. In this work steam exploded and torrefied woody biomass were studied with respect to NO_x formation in co-firing experiments. Most of the reported data is based on small scale experiments and simulations. In this work, however, have three different cases been investigated experimentally in a $1.5MW_{th}$ combustor supported by reaction simulations. One case corresponds to firing 100% Utah bituminous coal and two cases where 15% of the coal (on a mass basis) has been replaced with either torrefied or steam exploded biomass. Two of the cases was also studied in a utility scale $1.3\ GW_{th}$ industrial boiler. In both units did the case with pure coal result in the highest amount of NO formed, which was expected due to the higher amount of fuel-bound nitrogen in the coal, as compared to the biomass fuels. The fuel analyses indicate that the nitrogen content is the same in the two investigated biofuels. However, the amount of NO formed differed. Gas composition measurements reveal that the partitioning of volatile nitrogen species (HCN and NH_3) varies between the biomass co-firing cases. This was investigated further using detailed reaction simulations and is suggested as the main reason for the observed difference in NO formation.

1. Introduction

According to the Intergovernmental Panel on Climate Change, anthropogenic activities such as our use of fossil energy resources are proven to be the main cause for the climate changes that we are facing [1]. Large efforts are therefore invested to find alternative energy resources and to improve resource efficiency in order to reduce fossil fuel CO_2 emissions. One alternative that is discussed is the replacement of coal with bio-derived fuels. Another important emission apart from CO_2 that has received, and continues to receive, considerable attention due its negative effect on humans and the environment is nitrogen oxides (NO_X). An increased use of woody biomass fuels could potentially reduce the emission of both CO_2 and NO_X due to the generally lower nitrogen content and differing volatile contents. Co-combustion of biomass with coal is particularly attractive in order to mitigate the impacts of fuel mechanical properties and inorganic species in the ash [2–7]. Co-combustion of coal and biomass has been suggested to be one possible way to make the use of biomass for power production more efficient. One of the main reasons for this strategy would be to lower the problems

with aerosol formation and high-temperature corrosion otherwise related to combustion of biogenic fuels, but also for utilities to remain cost competitive with other electricity generation technologies; for example, gas-fired combined cycles [3,4]. Another consideration when switching from coal to biomass in metallurgical industries is to avoid any negative influence of ash chemistry on product quality. Applying co-combustion might then be a way to handle this and still be able to reduce CO_2 emissions in the range of 20–50%, depending upon the percentage of coal replaced with biomass.

Two sources of nitrogen can appear during combustion: N_2 from the air, and fuel-bound nitrogen, and NO may be formed from both sources. Depending on the form of nitrogen present, different general reaction routes are possible. The fuel-bound nitrogen is usually divided into the sub-categories of volatile-nitrogen (volatile-N) and char-bound nitrogen (char-N), reflecting the different ways in which nitrogen is bound to and released from the fuel. The NO_X formation form volatile-N can often be reduced significantly through effective burner design and the use of external air-staging. Since the char combusts relatively far from the burner, it is difficult to control the heterogeneous NO_x formation with

---

Table 1

Fuel compositions of the Utah bituminous coal and two thermally-treated biomasses. The table also includes the calculated composition of the mixtures used in the three cases investigated in this work. The composition is presented in % based on mass.

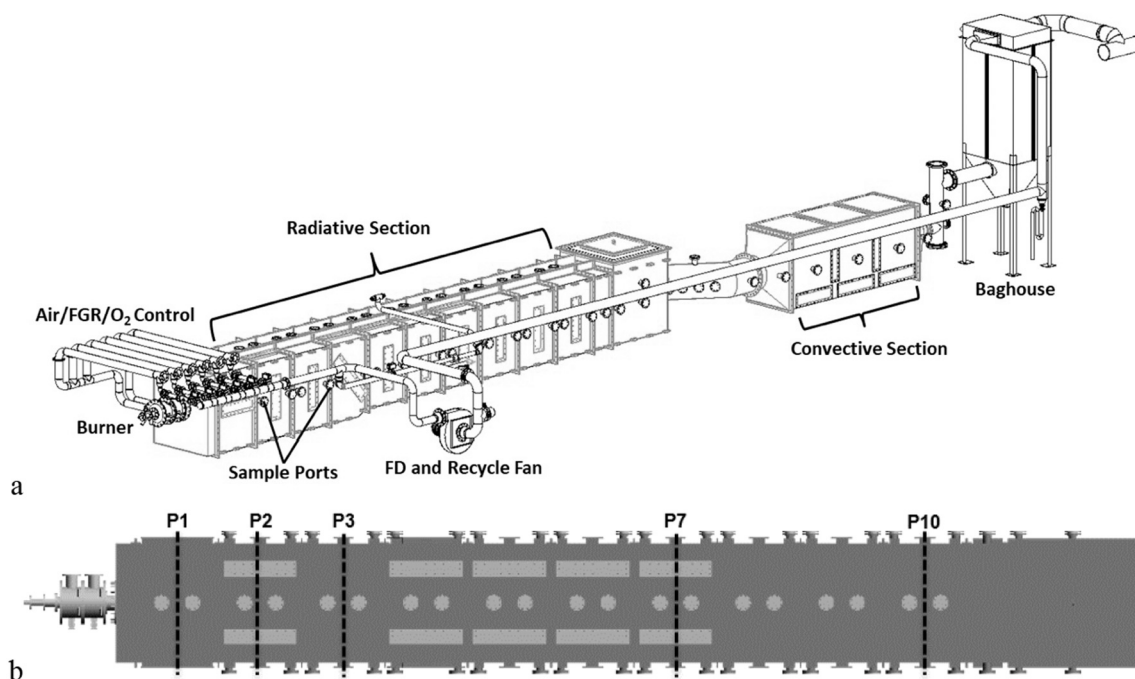| Fuel or case	Mixture	C	H	N	S	O	Ash	H_2O
Torrefied	–	54.98	5.16	0.59	0.00	29.60	7.44	2.24
Steam exploded	–	59.59	5.50	0.59	0.00	28.04	3.52	2.76
Coal	Utah bituminous coal (UBC)	61.48	4.47	0.91	0.58	12.21	16.20	4.15
Coal-T	UBC/Torrefied – 85/15	60.51	5.01	0.86	0.49	14.82	14.88	3.86
Coal-SX	UBC/Steam exploded - 85/15	61.20	5.07	0.86	0.49	14.58	14.29	3.94

Fig. 1. The 1.5 MW combustion unit located at University of Utah. The top figure (Fig. 1a) shows an isometric view of the unit and supporting hardware and the bottom figure (Fig. 1b) is a top view showing the four different port locations (P1-P3, P7 and P10) used for measurements in this work.

burner design. For this reason, the partitioning of nitrogen between volatiles and char is important [8–14]. Molina and co-workers [10] conducted a study on the reduction of NO in a drop-tube reactor and how the char and coal particles impacted the conversion of char nitrogen to NO. Their results, in line with previous findings, showed that the degree of char conversion reduces the nitrogen to NO transformation. Local stoichiometry, availability of oxygen also clearly influenced the conversion as did the background NO concentration. Spinti and Pershing [12] studied the fate of nitrogen during experiments with different coal-derived chars that were converted in lab-scale experiments in both air-fired and O2/CO2-based atmospheres. The test amtospheres were also doped with NOx up to concentrations of about 900 ppm. The parent coal impacted the conversion of char nitrogen to NOx and increased oxygen concentration increased the NOx formation. When the gas atmospheress were doped with NOx, this had an adverse effect on char nitrogen to NOx formation. Visona and Stanmore [13] performed single particle modeling studies to obtain information on NO formation from coal char. Different reaction paths were tested in the work using NO reduction kinetics form the literature. Direct reduction of NO on char or reduction via HCN proved equally relevant in the used modeling framework.

Riaza et al. [15] studied the volatile yield and the nitrogen partitioning of different biomass and coal types when using high-temperature pyrolysis conditions to generate chars. The observed difference in volatile yield between the coals and the white biomasses tested were noticeable. In general, the major part of the nitrogen in biomasses were released together with the volatiles (and not the char) while the coals presented a wider range in the fate of nitrogen from volatiles and char,

respectively. Data regarding the partitioning and release pattern of fuel nitrogen can be used to create a combustion environment the limits the formation NOX. For example will a flame with an oxygen-lean internal recirculation zone have low NO_x formation if most of the nitrogen is released with the volatiles, and a higher NO_x formation if most is retained in the char. Flames without an oxygen-lean internal recirculation zone can be expected to produce more NO_x if most nitrogen is released with the volatiles, since the net volatile nitrogen conversion to NO is typically more sensitive than the net char-bound nitrogen conversion to NO. [16,17] Studies have shown that volatile nitrogen release is enhanced at higher pyrolysis temperature. Although this is also true for carbon, nitrogen partitioning appears to be more sensitive to temperature [18]. The partitioning of the nitrogen is also dependent on how the nitrogen is bound in the fuel; something that varies between different fuel types such as coal and biomass. But it might also be affected by fuel pretreatment [14,15,19]. This work will investigate the influence of co-combustion of biomass and coal at two different scales, 1.5 MW_{th} and 1.3 GW_{th}. The aim is to study any differences from pure coal combustion with respect to NO_x formation. For this reason, steam-exploded and torrefied biomass have individually been co-combusted with Utah bituminous coal in a 1.5 MW_{th} combustion unit. The later mixture was also tested in 1.3 GW_{th} utility scale boiler. Further evaluation of the obtained data is performed using detailed reaction kinetic calculations aiming to find an explanation for the observed differences.

Table 2

Presented in the table is the type of data available for each case and port. G = gas composition data is available, T = temperature data is available.

	Coal	Coal-T	Coal-SX
Port 1	G/T	–	G/T
Port 2	G/T	G/T	G
Port 3	G/T	G*/T	G/T
Port 7	G/T**	G*/T**	G/T**
Port 10	T**	T**	T**
Flue gas	G	G	G

* Due to problems with the sampling in these positions all components and/or positions along the diameter might not be available.

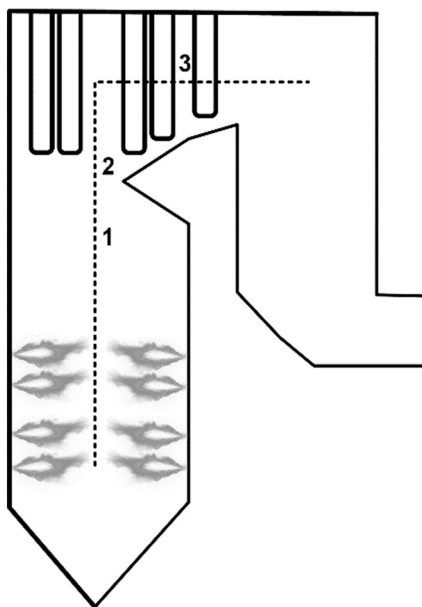** Only center position available

Fig. 2. Measurement position in the Hunter Unit 3 boiler. The dashed line indicates the path used to define the distance starting from the first burner row.

2. Methodology

The coal utilized in these experiments is Utah bituminous coal which has been combusted either pure or mixed 85/15 (on mass basis) with one of two biomass fuels, creating three different cases. Both biomass fuels originate from raw wood which was sourced in the Wasatch Mountains near Tibble Fork in American Fork Canyon in Utah, and the main species were pinyon pine (*Pinus edulis*), juniper (*Juniperus*) and spruce (*Picea*). The difference between the steam-exploded and torrefied biomass is how they have been treated to break down lignin and densify the energy. The material was shredded to a particle size of below 12 mm. The biomass was then treated via either steam explosion, at 20 bar with saturated steam, or through torrefaction at 325 °C. In the case of torrefaction, the shredded biomass was pelletized before the heat treatment. Following the pretreatment procedure, the fuels were blended and then pulverized in a Ramond 312 Bowl Mill in preparation for the pilot-scale experiments. The fuel composition for the pure fuels as well as the two fuel mixtures, coal with torrefied wood (Coal-T) and coal with steam-exploded biomass (Coal-SX), are shown in Table 1. The fuel composition, milling behavior, including resulting particle size distribution, was investigated as part of an earlier work by Dobó and Fry [2]. The fuel blends used in this work are chosen based on their work where more details can be found. Only one of the co-firing cases, Coal-T was used in the full-scale experiments.

The pilot-scale combustion experiments were carried out in the L1500 combustion unit located at University of Utah, shown in Fig. 1. The furnace is approximately 14.5 m (48′) long and has a square-shaped cross section with each side being approximately 104 cm (41″). The firing rate was approximately 880 kW$_{th}$ (3.0 MBtu/h) in all three cases. The air flow was adjusted to achieve a flue gas oxygen concentration of 3% on dry volume basis. The total air flow was divided between primary and secondary air registers in the burner and an over fire air (OFA) inlet located in the fourth section (Port 4) after the burner. Five of the available ports were used for measurements in the furnace. The temperature was measured along the diameter in Port 1, 2 and 3, as well as in the center position in Port 7 and 10 using a suction pyrometer. The same ports, except Port 10, were also used for gas composition measurements using a heated extractive sampling probe. The sampled gas was subsequently analyzed using an FTIR and a paramagnetic oxygen analyzer. Some of the main flue gas components have also been measured at the beginning of the convective section, which will be referred to as flue gas measurements. At this position, paramagnetic and NDIR analyzing equipment were used to determine the concentration of O_2 CO_2 and NO. Each experimental data point presented in this work is an average value based on a two-minute-long measurement. The actual measurement is initiated first after stable conditions has been reached. Unfortunately, gas composition and temperature data could not be obtained in all positions for all three cases investigated. Table 2 indicates the data that was obtained for each of the fuel conditions.

The full-scale utility measurements were conducted in Unit 3 at the Hunter Power plant in Castle Dale, Utah, operated by PacifiCorp. The unit has a thermal capacity of 1.3 GW but was operated at about 1.2 GW (4000 MBtu/h) during these tests. This unit incorporates a B&W wall-fired boiler and has burners installed at four levels on two opposing walls, as shown in the schematic drawing in Fig. 2. As mentioned earlier in the paper, only the torrefied wood pellets were used in the full-scale utility tests. The torrefied biomass was delivered to and mixed with the coal on site before entering the coal mills. The fuel mix used contained 15% biomass, the same percentage used in the pilot scale tests. This co-combustion test lasted for 24 h. The full-scale unit does not, for natural reasons, provide the same accessibility with respect to measurements and sampling. There were, however, three ports available for sampling which are marked as 1, 2 and 3 in Fig. 2. The first position is above the intake of the over fire air, position 2 above the "nose" and position 3 in between the super-heat and re-heat sections. The same sampling system and gas analyzers were used in the L1500 pilot-scale unit and the full-scale test. It was therefore only possible to measure about 2 m into the furnace and, due to the much larger size of the full-scale unit, not possible to reach all the way over to the opposing wall as it was in the pilot. The dashed line in Fig. 2 indicates the path used for determination of distance when comparing results between the pilot and full-scale unit. Note that the numbers used indicate "distance" of the measurement ports from the first burner row rather than their exact position.

The nitrogen chemistry in the L1500 unit was simulated in this work using a plug flow reactor (PFR) model in the software Chemkin. The detailed reaction mechanism used is a combination of different subsets found in the literature and includes the following: oxidation of hydrocarbons (C1–C3) [20–22]; nitrogen chemistry [23–25]; and sulfur chemistry [26,27]. There are some reactions suggested in the literature describing direct interaction between N and S species [28–30]. These reactions are often studied individually and/or under conditions that are different from those investigated in the present study, so no direct reactions between N and S species are included in this work. It should also be mentioned that the combination of subsets used in this work has not been validated as a combined mechanism. The purpose here was to discern general trends and perform a sensitivity analysis using a combination of experiments, rather than attempting to create a validated model. The same mechanism has been used before for similar purposes in previous work with satisfactory results [31]. The mechanism does, however, only include gas phase reactions, which is why a "fuel gas" representing the solid fuel was created that matches the experimental

Table 3
Fuel compositions, presented as mol fractions, used in the modeling work for each of the three cases.

	Coal$_M$	Coal-T$_M$	Coal-SX$_M$
HCN	0.0121	0.0117	0.0115
H$_2$S	0.0034	0.0029	0.0029
CH$_4$	0.2018	0.2110	0.2109
CO	0.7398	0.7337	0.7336
H$_2$O	0.0429	0.0407	0.0411

Table 4
Cases used to investigate the influence of residence time and temperature.

Case	Base	Temperature profile	Velocity profile
Coal$_M$	Coal$_M$	Coal$_M$	Coal$_M$
Coal-T$_M$	Coal-T$_M$	Coal-T$_M$	Coal-T$_M$
Sensitivity 3	Coal-T$_M$	Coal$_M$	–
Sensitivity 4	Coal-T$_M$	Coal-T$_M$	Coal$_M$
Sensitivity 5	Coal-T$_M$	Coal$_M$	Coal-T$_M$

fuel analysis. This fuel gas was creating by assuming the following;

- moisture is introduced as H$_2$O.
- N is introduced as HCN
- S is introduced as H$_2$S
- The remaining amount of H is introduced as CH$_4$.
- The remaining C is introduced as CO.
- If more O is required in order to fulfil what is stated above, the amount of oxygen introduced via the air has been adjusted accordingly keeping the total mass flow of each element the same as in the experiments.

The resulting gas composition for each case is presented in Table 3. To be able to distinguish between experiments and modeling, the modeling cases are market with "M." Note that oxygen had to be added to the fuel mix in all three models to fulfil the assumptions listed above. For Coal$_M$, Coal-T$_M$ and Coal-SX$_M$, about 24%, 28% and 27% respectively of the oxygen content presented in Table 3 originated from the actual fuel.

The temperature in the PFR was set using a fixed temperature profile based on the temperatures measured along the center line of the L1500 unit during the experiments. The inlet temperature was set to 260 °C in all cases which was the set inlet temperature in the secondary air fed to the burner. As presented in Table 2, there are some temperature data missing for Coal-T and Coal-SX. The missing temperature for Coal-T$_M$ in port 2 is therefore assumed to be the same as for Coal$_M$ in the same port. The same assumption is made for Coal-SX$_M$ in port 2 and 3. The temperature profile after Port 10 (1220 cm) is an extrapolation of the temperature decrease between Port 7 and 10. The importance of temperature will also be investigated as part of a sensitivity analysis.

Injection profiles have been used for both air and fuel in order to compensate for the radial mixing resistance of fuel and air caused by burner aerodynamics, which does not exist in a PFR. The use of injection profiles for this purpose have been used previously and are shown to be able to describe the combustion sufficiently for the model to capture important parts of the related chemistry [32–34]. The method can be applied for different combustion systems, but the actual injection profiles have to be adjusted for each specific combustion environment. The cumulative profiles used in this work are shown in Fig. 4a and b for fuel and air, respectively. Note that the air injection profile includes all air supplied, including the OFA. Both profiles are determined by fitting the simulated O$_2$ and CO profiles with the measured concentrations of the same components along the centerline in the L1500 unit. The same cumulative injection profiles have been used for all three cases with only the absolute amount, and composition, of fuel and air being adjusted.

There is also a linear injection profile for fuel presented in Fig. 4a. This alternative profile was, however, only used as part of the sensitivity analysis. During this sensitivity analysis, the nitrogen containing part of the fuel is introduced separately using the alternative injection profile, while the remaining part of the fuel still follows the main fuel injection profile. The separated nitrogen content was then introduced as either HCN (Sensitivity 1), same as in the main models, or NH$_3$ (Sensitivity 2).

In another sensitivity analysis, the influence of temperature and residence time was investigated. In the main model the geometry of the PFR is set. Any eventual differences in volumetric flow would therefore also result in a different velocity and residence time. To investigate how this is influencing the chemistry, the temperature and resulting velocity profile from the Coal$_M$ case was applied individually and together to the Coal-T$_M$ case. This resulted in three different sensitivity cases, listed in Table 4.

3. Results

Utah Bituminous coal is combusted alone and together with biomass that has been thermally treated via either torrefaction or steam explosion creating three cases: Coal, Coal-T and Coal-SX. All three cases were combusted in the L-1500 research combustor, but full-scale tests were only conducted on Coal and Coal-T at Hunter, Unit 3. Fig. 5 shows the flue gas NO concentration measured for all cases available. The concentrations have been normalized with respect to the reference case, the Coal case, in each respective combustion unit. The figure shows notable differences when firing each of the fuel and fuel blends. The data in Table 1 shows that the bituminous coal has a higher nitrogen content than the two biomasses, which is why it is reasonable that the highest NO concentration is found for that case. Table 1 also shows that the nitrogen content is the same for both biomasses, and, based on only the nitrogen content, there should be a reduction in NO of 6.5% for the Coal-T and Coal-SX cases compared to the reference Coal case. The data in Fig. 5 shows that this is almost the case for Coal-SX which has a reduction of 8% compared to the Coal case. The Coal-T case, on the other hand, has a much higher reduction in NO concentration, with 30% in the L-1500 unit and 15% in Hunter. Both of these reductions are significantly larger than that suggested by the nitrogen content in the fuel indicating that the mechanism for NO formation is much more complex than only fuel nitrogen content. Additional measurements were performed to investigate this further and supporting detailed chemical reaction simulations were performed. The results are presented in the following sections.

3.1. Comparing pilot and full scale

As shown in Fig. 5, there was a similar trend with reduced flue gas concentration of NO due to the addition of torrefied wood in the full-scale unit and in the pilot unit. In this section, gas composition measurements from within the two units are compared. Note that the L-1500 unit is not designed to be an exact down-scaled model of the full-scale unit, which is why the normalized distance used in the discussion below (diameter over length) is different for each unit, with the research combustor longer and narrower. There are also differences in accessibility between the two units. The concentrations shown in this section for the L-1500 unit are average concentrations measured over the horizontal center line in each port used. This was not possible in the full-scale unit, instead the included averages are based on our measurements between 0.75 m and 1.75 m into the furnace in the ports used. Another difference worth noting is that the first measurement from the pilot-scale unit used in this comparison, port 3, is slightly before the OFA injection. On the other hand, position 1 in the full-scale unit is downstream of the OFA.

Fig. 6 presents oxygen and carbon monoxide concentrations measured in both units. It can be seen in the presented data that complete combustion was not reached in the first position but was reached in
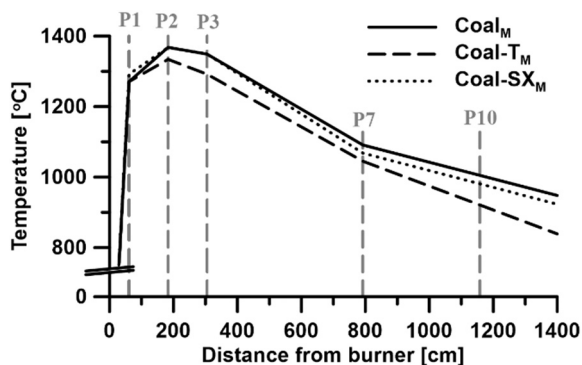
Fig. 3. Temperature profiles used in each of the three simulated cases.

the final position. Despite the large differences in the two units, the data presented here is represents the same conditions, namely the transition from the late combustion zone into the post-combustion zone. The concentration of oxygen and carbon monoxide is relatively similar between the two cases for both units with one possible exception being the CO concentration in the L-1500 unit. Here it seems that the combustion is a bit slower in Coal-T case based on the higher CO concentration. The later concentrations, however, are similar.

The trends for the Coal and Coal-T cases are similar with respect to the volatile nitrogen species, HCN and NH_3, even though the absolute concentrations are different. In the L-1500 unit, the concentration of both components is about four times higher in the Coal case compared to the Coal-T case, as shown in Fig. 7. A similar difference is also seen with respect to HCN in the full-scale unit. With respect to NH_3, on the other hand, the difference between the two cases is much smaller and the Coal-T case has the higher concentration. The NH_3 concentration profile for the full-scale unit also differs from the other profiles shown in Fig. 7 by the fact that it is not continuously decreasing. Instead, there is an increase found between the second and third measurement position.

3.2. Pilot scale

Detailed measurements were performed in the L-1500 pilot-scale unit including temperature and gas composition measured in Ports 1, 2, 3, 7 and 10, according to Table 2. The temperature data obtained is presented in Fig. 8. The Coal case was the only case where the temperature was measured in all three ports closest to the burner. A color map based on these temperatures is presented in Fig. 8a showing the temperature distribution of the flame. Each specific experimental data point used is marked with "*" in the figure. Most of the flame zone is at a temperature between 1250 °C and 1400 °C. Plots comparing the temperature profile measured in the Coal case and the available data for the biomass blend firing conditions are presented in Fig. 8b. The

temperature profiles seem to be similar during co-combustion as for combustion of pure bituminous coal. The largest discrepancy is found in Port 3 where the temperature in the Coal-T case is lower than in the Coal case. The average temperature is, however, less than 30 °C higher in the latter case. A comparison between the temperatures measured in center position Port 7 and 10 is not presented here. They do, however, follow the same trend with the Coal-T temperature being the lowest and the other two more or less the same as can be seen in Fig. 3 by comparing the temperature profiles used in the models. It should also be mentioned that the thermal properties of walls and cooling surfaces might change over time due to depositions and may influence the temperature profile, in addition to the operating conditions and combustion properties.

Oxygen and CO concentration profiles are presented in Fig. 9 and show that oxygen distribution is similar for Coal, Coal-T and Coal-SX in all four ports measured. Especially in Port 2 and 3, the oxygen levels are very similar between the three cases. In Port 1, however, there is a somewhat lower oxygen concentration in the Coal-SX case compared to the Coal case. This is consistent with the CO profiles where the concentration of carbon monoxide is higher in Port 1 for Coal-SX compared to the Coal case. Here it can also be seen that even though the O_2 profiles are similar in Port 2, the CO concentration is lower in the Coal-SX case compared to the other two, which are very similar. In Port 3 the levels are again similar. In this port, it is Coal-T that has a slightly higher CO concentration compared to the other two, even though the difference is small. It should also be mentioned that there is a notable relative difference in CO concentration between the three cases in Port 7. The concentrations are, however, in ppm-level instead on percentage which makes the absolute difference much smaller than what has been seen in the other ports.

As shown in Fig. 10, near the burner (Port 1) the concentration of methane is higher in the Coal-SX case compared to the Coal case. In Port 2 and 3, on the other hand, the methane concentration is lower
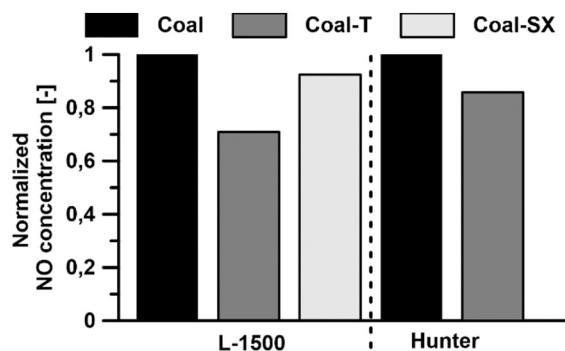

Fig. 5. Flue gas concentration of NO in the three investigated cases, pure coal as well as coal with 15% torrefied and steam-exploded wood, respectively.
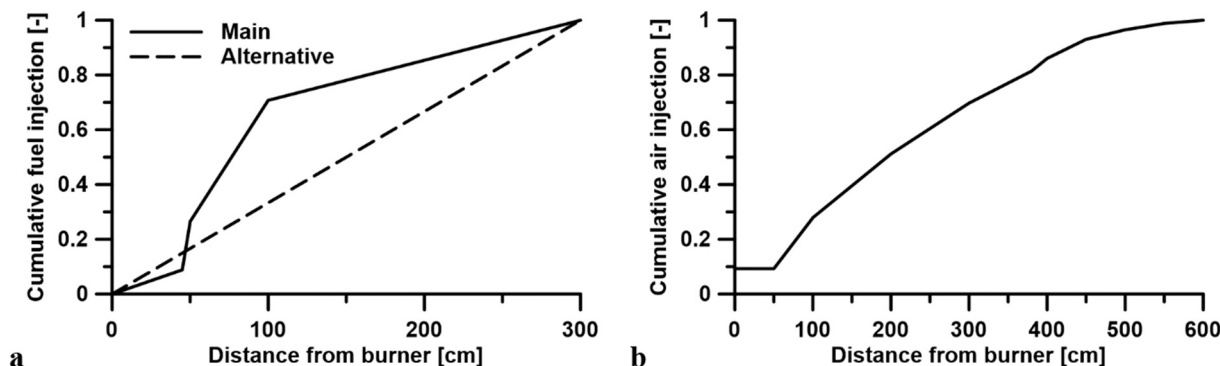

Fig. 4. Cumulative injection profiles for fuel (Fig. 4a) and air (Fig. 4b). The "Main" profile is the profile used in the main model and the "alternative" linear profile is only partly used in the sensitivity analysis.
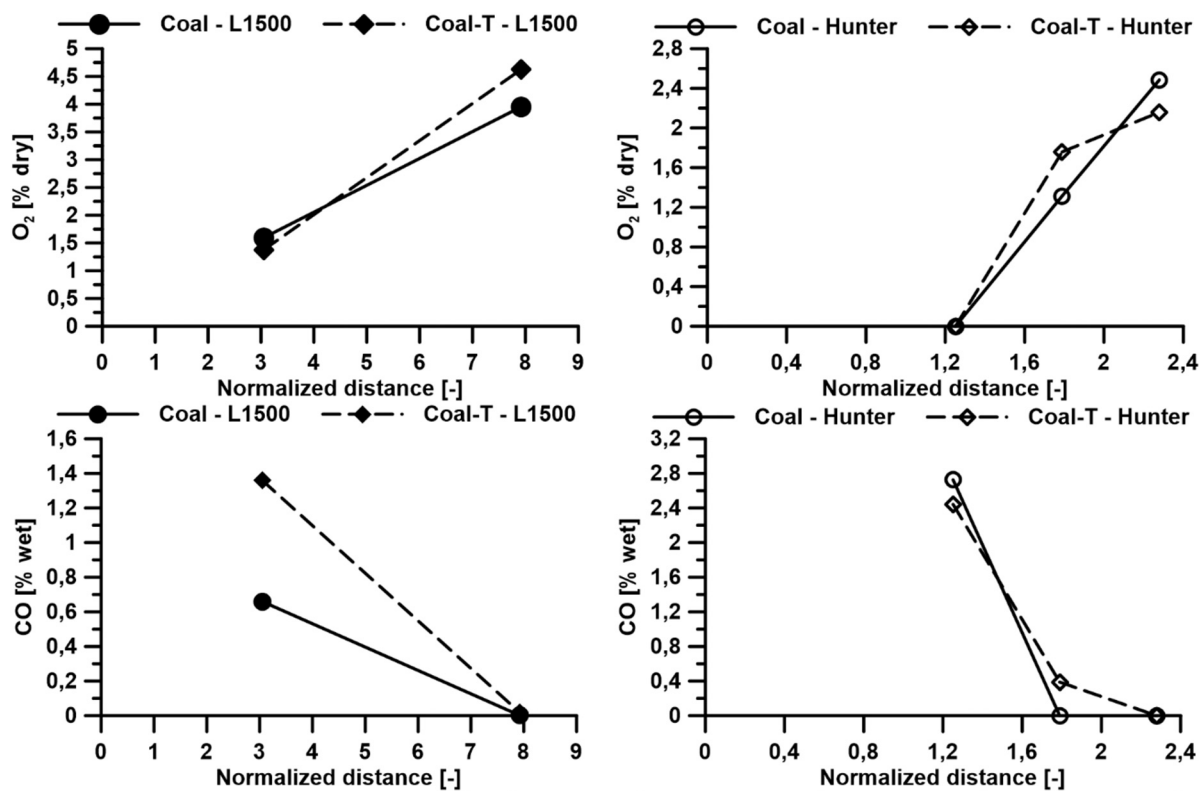
Fig. 6. Oxygen concentration, top row, and carbon monoxide concentration, bottom row, with respect to normalized distance on both the pilot, L-1500, and full-scale unit, Hunter.
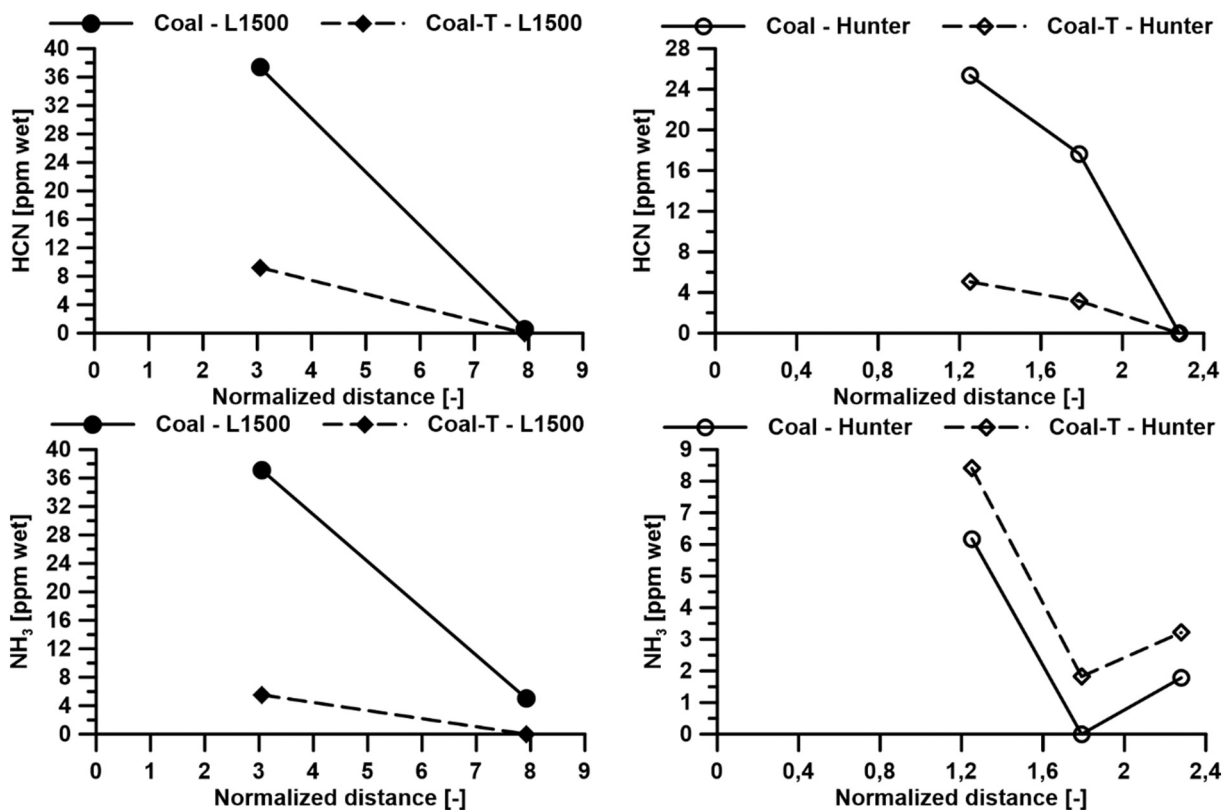

Fig. 7. HCN concentration, top row, and NH$_3$ concentration, bottom row, with respect to normalized distance on both the pilot, L-1500, and full-scale unit, Hunter.
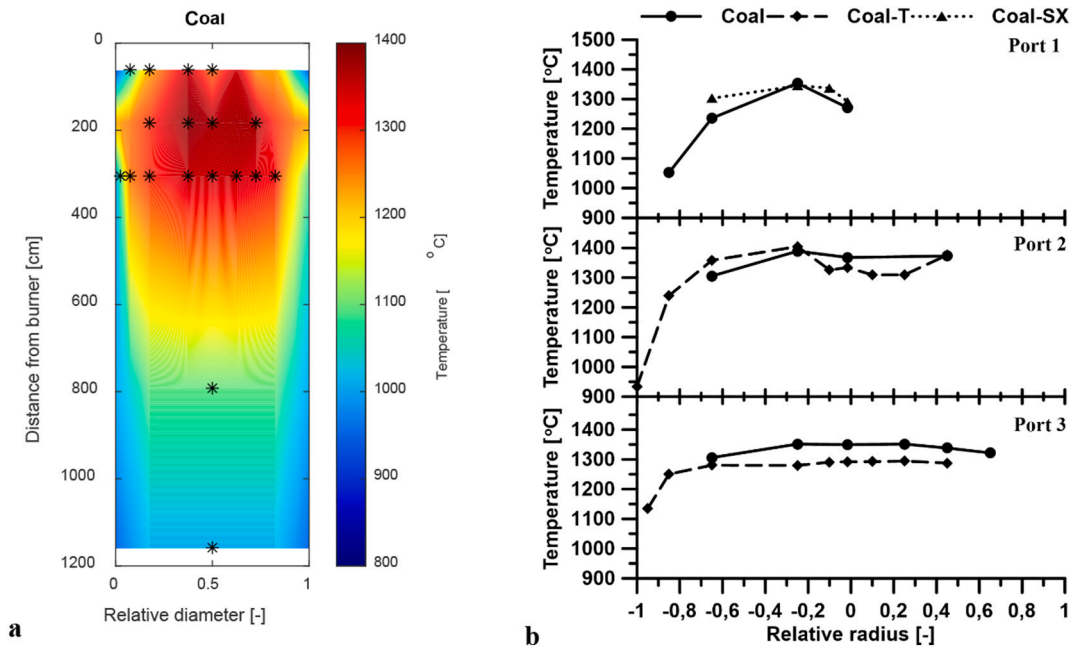
Fig. 8. Temperature data for the different cases. Fig. 8a is a color map based on temperature measurement from the Coal case. "*" marks the positions where the temperature has been measured. Fig. 8b presents a comparison between the available data for all three cases in port 1(top), port 2, (middle) and port 3 (bottom).
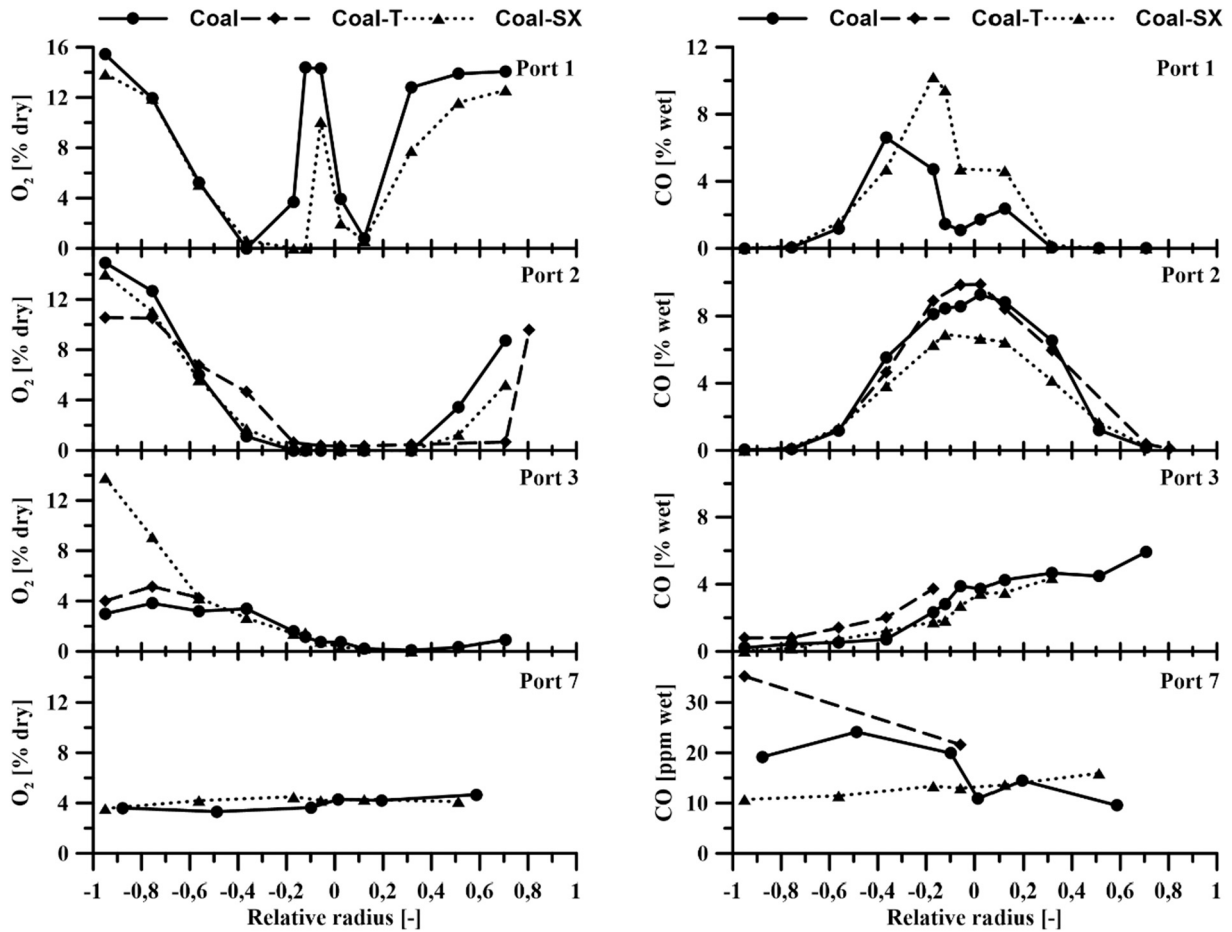

Fig. 9. Oxygen concentration (to the left) and CO concentration (to the right) for all three cases investigated. The different rows represent Port 1, 2, 3 and 7 respectively. Note that the why axis in CO figure for port 7 (bottom row) has a different unit, ppm wet instead of % wet.
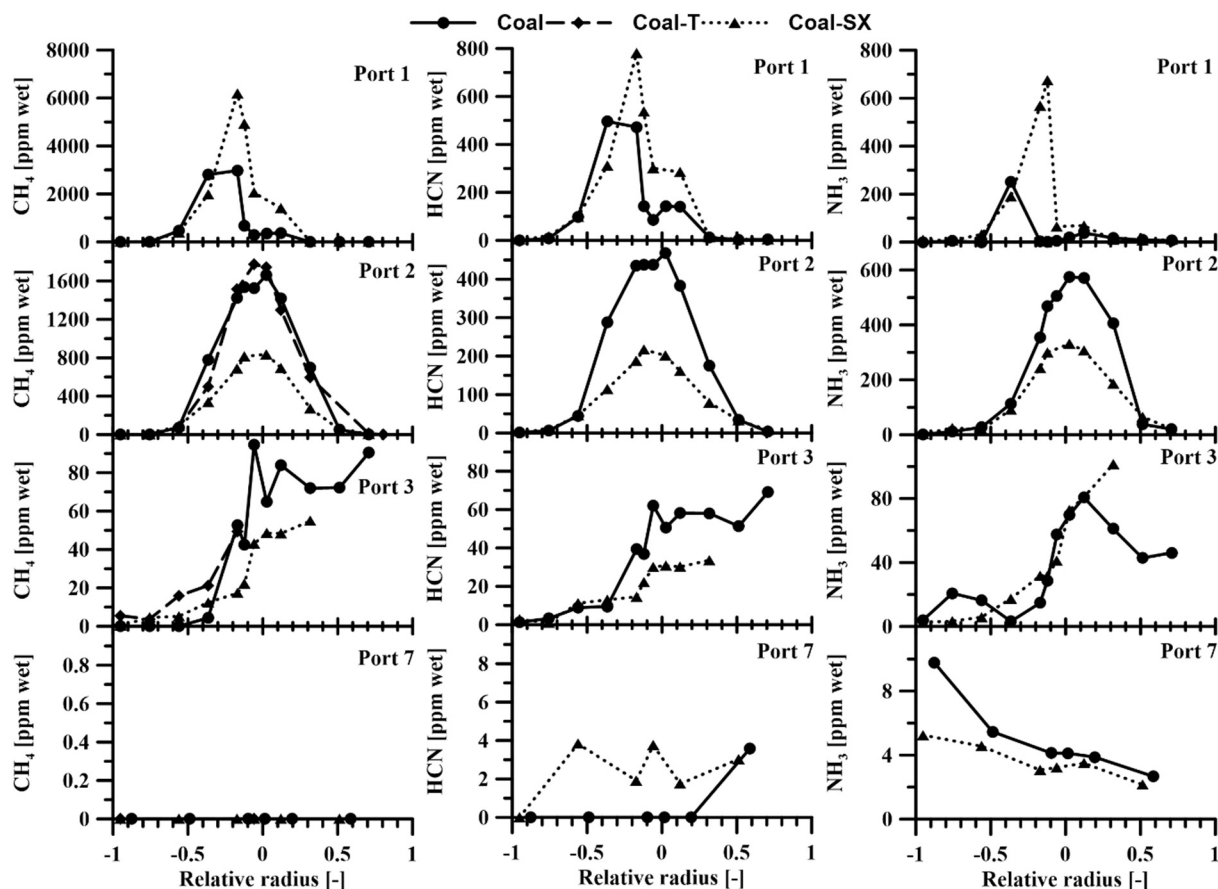
Fig. 10. CH_4 (to the left), HCN (in the middle) and NH_3 concentration (to the right) for all three cases investigated. The different rows represent Port 1, 2, 3 and 7, respectively. Note that there is neither HCN nor NH_3 data presented for the Coal-T case.

compared to both the Coal and Coal-T case. For the volatile nitrogen species, also in Fig. 10, there is again a relatively large difference between the Coal and Coal-SX case, with higher concentrations for Coal-SX in port 1 and the opposite in port 2.

3.3. Simulations

Each of the three cases investigated experimentally in the L-1500 unit were simulated using a detailed gas phase reaction mechanism implemented using a PFR model in the software Chemkin. As mentioned in the methodology section, the air and fuel injection profiles were created by fitting the simulations to experimental data with respect to O_2 and CO in the reference case, Coal. Fig. 11 provides a comparison of model predictions with O_2 and CO data. The top row of figures presents the comparison between simulations and experiments for baseline Coal case. For this case the CO concentration is first linearly increasing until it momentarily went to nearly zero and then increased to around 16%. A similar trend, but with an initial linear reduction, can also be seen for O_2. This discontinuity is a result of ignition behavior in the model. When a certain composition and temperature is reached most of the combustibles and oxygen are consumed, causing the downward spike in CO concentration. Meanwhile, the injection of both air and fuel continues with a faster injection of fuel creating a fuel rich environment. This fuel rich environment lasts until a distance from the reactor inlet of 375 cm, 75 cm after the end of the fuel injection profile. Once all the fuel has been oxidized there is an increase in O_2. This behavior does not accurately describe real heterogeneous reaction profiles of solid fuel, but is sufficient to provide an accurate environment for studying the chemistry of interest here. As mentioned in the methodology section, the injection profiles are tuned to get a good agreement between the modeled case,

$Coal_M$, and the experimental data, Coal, with respect to CO and O_2. The same air and fuel injection profiles where also used for Coal-T_M and Coal-SX_M but with the absolute values adjusted corresponding to the change in fuel composition. Despite the relatively small changes in fuel composition, due to only 15% of biomass in the blends, there were some clear differences in O_2 and CO observed during the experiments. The agreement between experiments and simulations was also found for the other cases, Coal-T and Coal-T_M as well as Coal-SX and Coal-SX_M respectively (see middle and bottom rows of Fig. 11).

The good agreement between experiments and simulations presented in Fig. 11 should be expected, especially for Coal and $Coal_M$, on which the injection profiles were created. The model does, however, also agree with the experiments with respect to NO, which is presented in Fig. 12. All the NO concentrations shown here are normalized with respect to the outlet NO concentration in the Coal case. As can be seen, there is a peak in NO concentration around the point of ignition for the three modeled cases. High early concentrations were also found experimentally in the Coal and Coal-SX cases. The plot in the bottom right corner of Fig. 12 is a comparison between the three modeled cases with the first 100 cm excluded to avoid the initial peak and focus on post ignition behavior.

Fig. 13 presents measured and simulated concentration profiles of NH_3 and HCN for each of the three fuel cases. The simulations suggest a peak in NH_3 concentration, to the left in Fig. 13, in connection with the earlier mentioned ignition point. The peak value is more or less the same in all three modeled cases. In $Coal_M$ and Coal-T_M this value is also similar in magnitude to the peak concentration in the respective experimental case, but the measured concentration is lower for the Coal-SX case than the model suggests. However, it should be noted that the data point in question is on a steep concentration gradient with respect to furnace
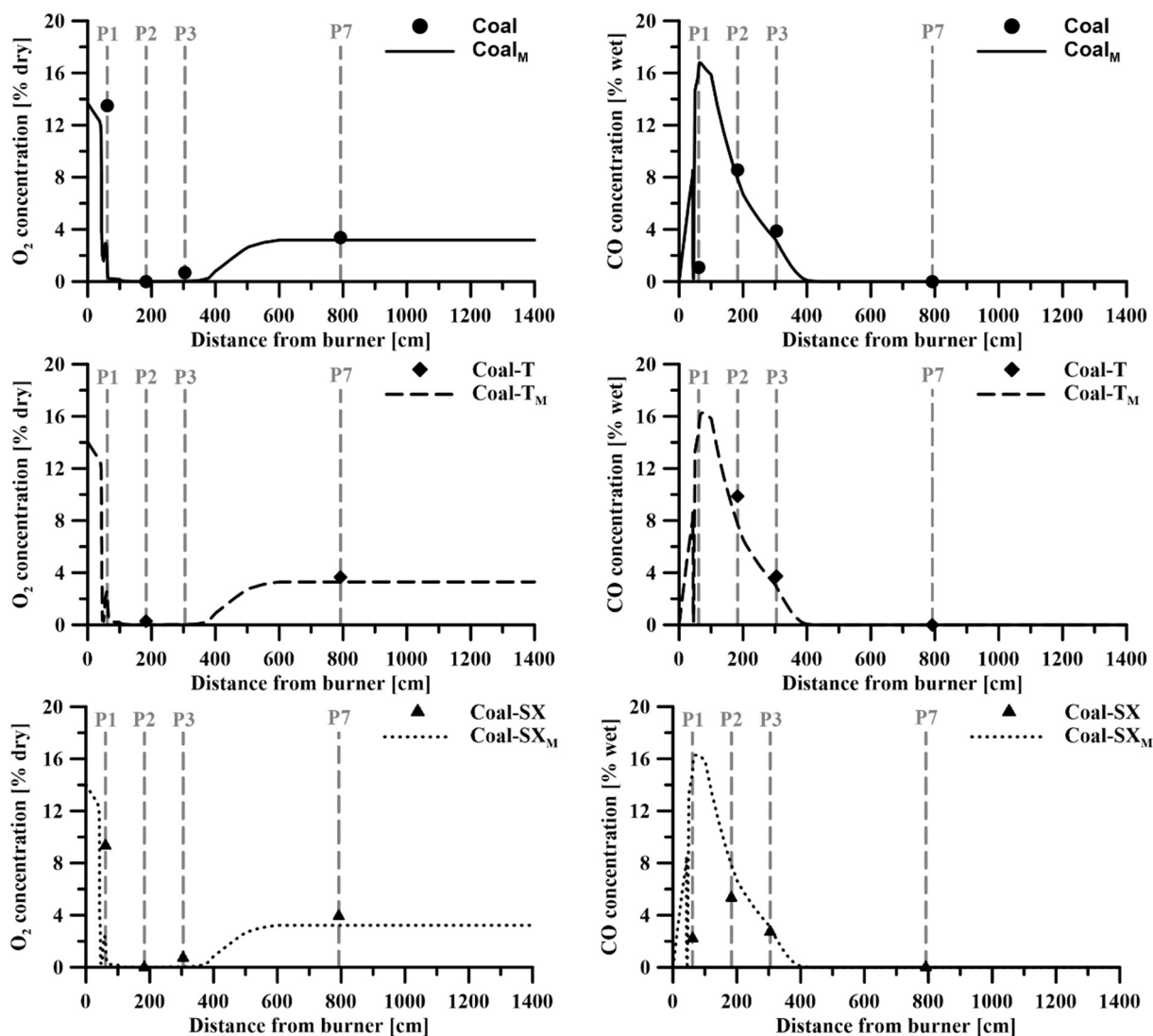
Fig. 11. Comparison between measured and simulated O_2 and CO concentrations in the L-1500. The experimental results are indicated by symbols and the simulation results by continues lines.

position/temperature.

3.4. Sensitivity analysis

As shown in Table 3, all fuel-bound nitrogen is assumed in the simulations to be released as HCN. The fuel is also injected following one injection profile. As part of the sensitivity analysis, it was tested to separate the nitrogen content from the main fuel input and inject it according to the linear injection profile shown in Fig. 4a. This profile was used to introduce all nitrogen both as HCN, Sensitivity 1, and NH_3, Sensitivity 2. These tests are based on the $Coal_M$ case and are therefore compared to the same in Fig. 14, which shows that the linear profile results in a much higher formation of NO. The difference between introducing the fuel bound nitrogen as HCN or NH_3 is on the other hand minor. As a second part of the sensitivity analysis, temperature and residence time were examined. Table 4 presents three sensitivity simulations, Sensitivity 3, 4 and 5, where the temperature and velocity of the $Coal_M$ case were applied to the Coal-T_M case. The results from each of these three simulations as well as the original cases are presented in Fig. 15. Sensitivity 4, which had a temperature profile from the Coal-T_M case and velocity from the $Coal_M$ case, is slightly higher compared to the Coal-T_M case. Sensitivity 3 which was based on the $Coal_M$ temperature profile only had a slightly higher NO concentration compared to the

$Coal_M$ case. Sensitivity 5 had both velocity and temperature profile from the $Coal_M$ case and produced an almost identical result, which is why the corresponding line cannot be seen behind the $Coal_M$ line.

4. Discussion

It was shown in Fig. 5 that co-combustion of thermally treated biomass with coal can lower the NO emissions compared to combustion of pure coal. It also became evident that the reduction in NO formation is larger than the difference in nitrogen content between the two fuels. That co-combustion of biomass and coal can result a change in NO formation, compared to combustion of pure coal, that does not directly correlate to the difference in fuel-bound nitrogen has also been reported in experimental and modeling work by Wang et al. [35] and Tu et al. [6] respectively. Based on this work it also became clear that not only the nitrogen content but also the type of pretreatment used for the biomass also has an influence on the NO formation. This was investigated further by performing in-flame measurements of both gas composition and temperature in the L-1500, pilot scale unit. Even though that unit is not a down-scaled version of the Hunter power plant Unit 3, the two tests still showed overall similarities with respect to NO formation and overall combustion, which is important in connection with the nitrogen chemistry. It is therefore assumed that knowledge obtained from the pilot-
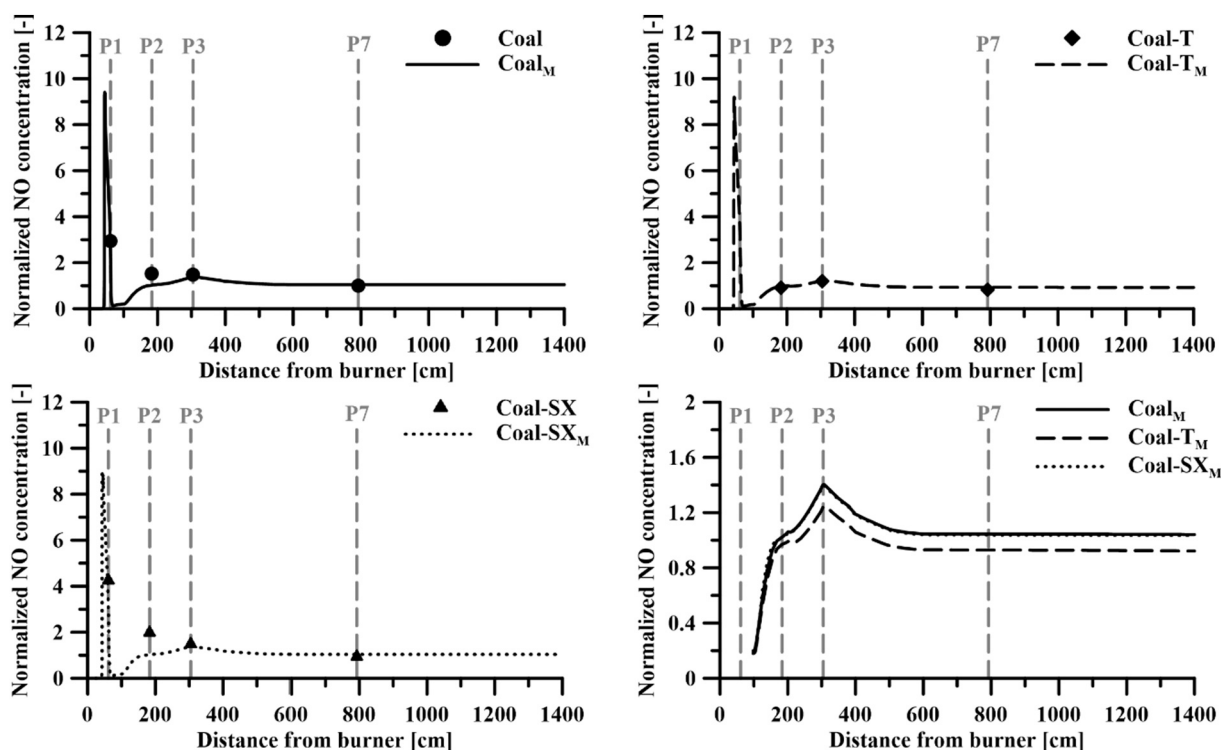
Fig. 12. Comparison between results from L-1500 experiments and simulation for the three cases investigated. All NO concentrations are normalized with respect to the Coal case outlet concentration. Note also that the figure to the bottom right does not contain any information at distances between 0 cm and 100 cm.

scale unit, and simulations of the same, can be applicable to the full-scale unit. The model is shown to be capable of capturing the general trend seen in the experiments and, at least partly, to capture the difference found in NO concentrations of the three fuels. Both Coal-T$_M$ and Coal-SX$_M$ have a lower outlet NO concentration than Coal$_M$. For the Coal-SX$_M$ case, the difference is small and barely visible in the figure while there is a clear difference found between Coal$_M$ and Coal-T$_M$. A larger difference between Coal$_M$ and Coal-T$_M$ compared to the difference between Coal$_M$ and Coal-SX$_M$ is consistent with the measured outlet NO concentrations for the three cases presented in Fig. 5.

Fig. 9 showed that the Coal-SX case differed from the other cases with respect to CO concentration, but it is also different with respect to methane, seen in Fig. 10. This is an indication that there are some differences in volatilization between the cases. This is in agreement with what is seen for the HCN and NH$_3$, Fig. 10. For these species, there is again a relatively large difference between the Coal and Coal-SX case with higher concentrations for Coal-SX in port 1 and the opposite in port 2. The reason for this could be the same as for why the CH$_4$ concentration is different; namely, that the volatile matter is released earlier in the Coal-SX case. The NH$_3$ concentration is, however, higher again in Port 3 for the Coal-SX case. This is something that is not seen for HCN suggesting that there might be a secondary formation of NH$_3$ independent of the formation of HCN. The lowest concentration of NO was measured in the Coal-T case, which was represented well by the model. A deeper understanding of this behavior is required because its cause is not immediately apparent. The nitrogen content is the same in both biomass fuels, thus the amount of fuel bound nitrogen is not the cause. One possibility is, however, that the nitrogen is bound differently in the fuel, which may be a result of the two different pre-treatments, which may influence the release of nitrogen. A difference in carbon monoxide and methane, as well as for HCN and NH$_3$ concentrations, between the cases was observed in the experiments. This suggests that the release of volatile matter might be different.

Even though differences were found in the measured concentrations of NH$_3$ and HCN, this was not the case for the simulated cases as shown

in Fig. 13. The simulations suggest an early peak in NH$_3$ in connection with the ignition point in the model. The peak value is more or less the same in all three modeled cases. In Coal$_M$ and Coal-T$_M$, this value is also similar to the peak concentration in the respective experimental case, but the measured concentration is lower for the Coal-SX case than the model suggests; however, the data point in question is on a steep concentration gradient with respect to furnace position/temperature. Experiments and simulation both suggest an early peak in NH$_3$ concentration. A similar trend with an initial peak is seen in both experiments and simulations with respect to HCN. There are, however, differences between the model in exact position and shape of these peeks. The differences could be caused by the characteristics of the model, assuming for example perfect radial mixing and all fuel-N in the form of HCN. These settings have to be kept in mind when comparing results from the model and experiments.

The different ways of introducing fuels during co-combustion can influence the formation of NO. In this work the importance of fuel injection was investigated as part of the sensitivity analysis presented in Fig. 14 which indicates a clear effect of the different injection profile, which goes in line with what has been reported by others [6,36–38]. Of the two profiles investigated in this work is the linear injection profile resulting in a much higher outlet NO concentration. The main difference between the two profiles is that about 70% of the nitrogen is introduced between a distance of 100 cm and 300 cm from the burner for the linear profile, compared to 30% in the main fuel injection profile. This region is after the reduction of all the initially formed NO and where most of the NO actually leaving the rector is formed. The difference between introducing the fuel bound nitrogen as HCN or NH$_3$ is on the other hand only minor. This result shows that when and at what conditions the volatile nitrogen species are released does matter and could potentially have a large influence on the overall NO formation. Riaza et al. [15] investigated six different fuels, three coals and three biomasses, during high temperature pyrolysis. Their results showed, on one hand, a clear difference in nitrogen partitioning between the fuels, but also that the release of volatile nitrogen was higher for all fuels during high
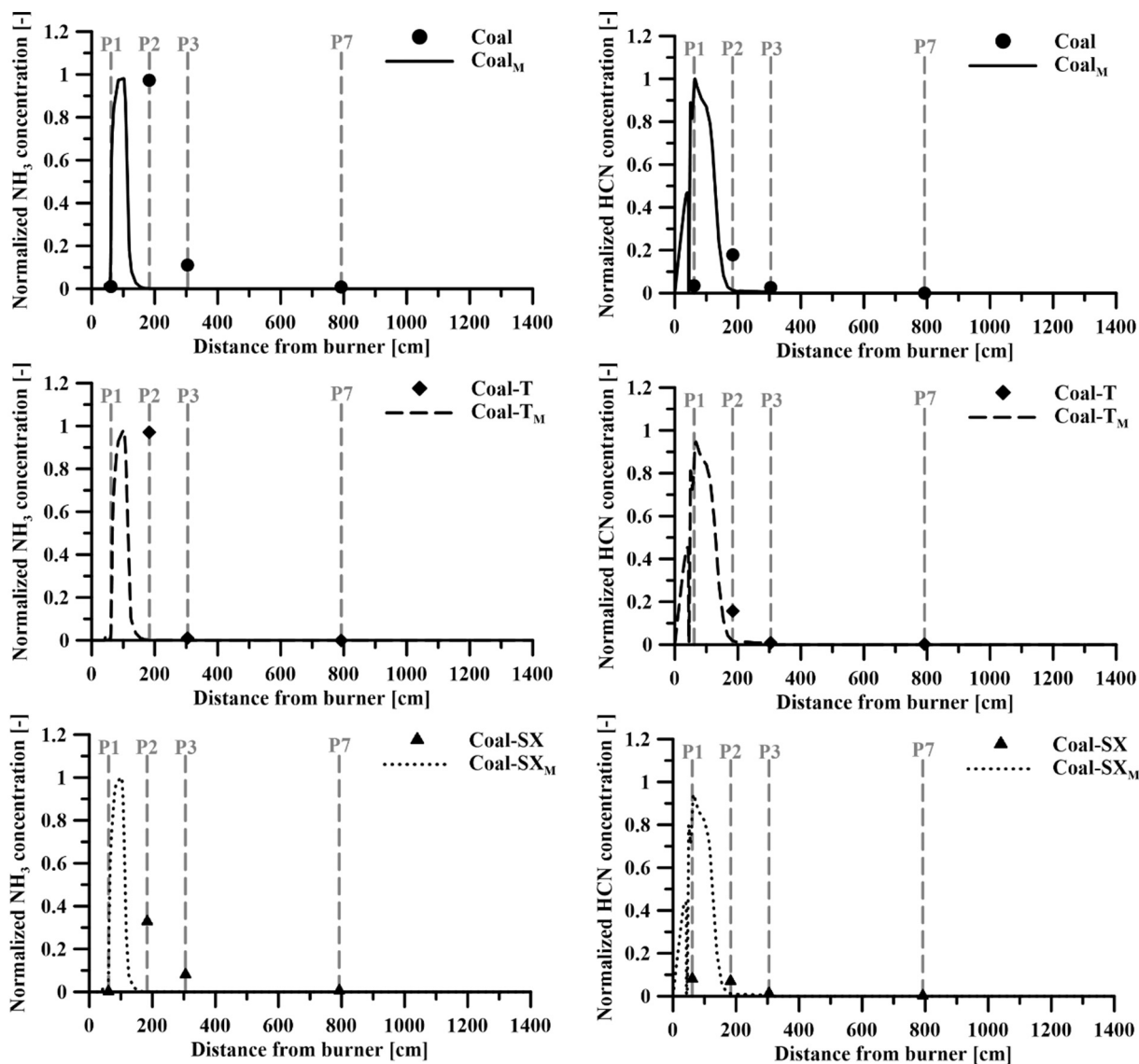
Fig. 13. Comparison between simulated and measured NH_3, to the left, and HCN, to the right, concentrations from the L-1500. The concentrations are normalized with respect to the highest NH_3 and HCN concentration respectively among all cases.
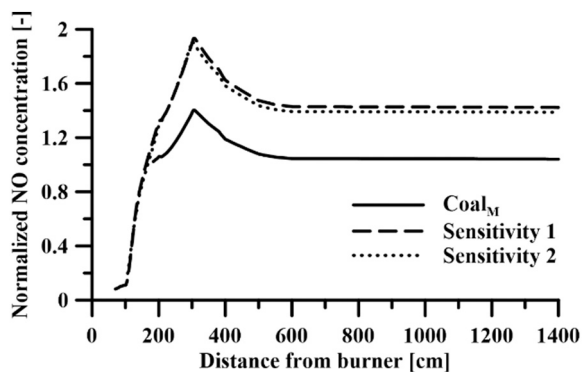

Fig. 14. The influence of injecting the nitrogen according to a linear injection profile and by introducing the fuel bound nitrogen as HCN, Sensitivity 1, or NH_3, Sensitivity 2.
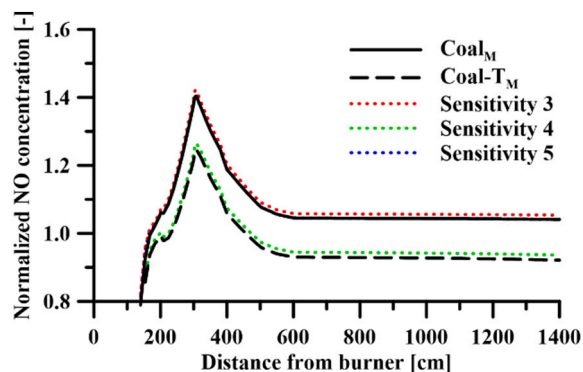

Fig. 15. Results from the sensitivity analysis looking at the influence of temperature and residence time on NO formation.

temperature pyrolysis compared to what was given by a proximate fuel analysis. This increase was, however, not the same for all fuels. This result goes in hand with the results from this work showing that the

reduction in NO emissions is not directly proportional to the lower nitrogen content shown in the fuel analysis. Even though it did not seem to be important if the nitrogen is released as HCN or NH_3 based on the sensitivity analysis, there could be some indirect effects. As shown in Fig. 12, there are some differences in HCN and NH_3 concentration trends suggesting differences in their respective release pattern. If one tends to be released during certain conditions, it could potentially result in an indirect effect related to whether the nitrogen is released as HCN or NH_3. This proposed by Tu et al. [6] in their work to be the explanation to why the NO formation changed depending at what burner level the biomass was introduced to the boiler.

The fuel particle size distribution (PSD) is also an important parameter that effects the combustion. A smaller particle will be heated up faster than a larger particle, resulting in a faster devolatilization and possibly more intense combustion with higher temperatures. The milling performance of the same fuels investigated here was investigated in a previous work by Dobó and Fry [2]. According to their findings, co-milling of coal and steam-exploded pellets had the particle size distribution that was most similar to the one for pure coal. The Coal-T mix did, on the other hand, result in an increase of larger particles. This change could be a reason for the difference found in e.g. CO concentration in the flame. The biomass fuels are more volatile compared to the coal, and a biomass particle of the same size as a coal particle will devolatize faster compared to the coal particle, which is indicated by the higher CO, HCN and NH_3 concentrations found early for the Coal-SX case (Figs. 9 and 10). The same reasoning could then be used to explain the similarities between the Coal and Coal-T case. The slightly larger particles in the Coal-T case are partly compensated by the biomass content but are still resulting in a partly delayed combustion, which was seen in both the pilot- and full scale- unit. A delayed combustion could increase the residence time during which already-formed NO could be reduced again.

As mentioned earlier, the temperature is also an important parameter that is connected to the combustion and formation of NO. There were some differences in temperature observed during the experiments between the cases which were also described in the simulations, as shown in Fig. 3. The temperature could potentially affect the simulations by the temperature dependence in the reaction kinetics. The same PFR geometry was used in in all three cases, $Coal_M$, $Coal-T_M$ and $Coal-SX_M$, which causes an indirect effect of temperature on the velocity, and hence also the residence time. The influence of temperature and residence time was examined as part of the sensitivity analysis. Table 4 presents three sensitivity simulations, Sensitivity 3, 4 and 5, where the temperature and velocity of the $Coal_M$ case were applied to the $Coal-T_M$ case. The results from each of these three simulations as well as the original cases are presented in Fig. 15. In Simulation 3, the $Coal_M$ temperature profile is applied to the $Coal-T_M$ case and as can be seen this results in the same NO concentration as in $Coal_M$. But in this case, it is then not only the temperature but also the residence time that has changed. In Sensitivity 4, the $Coal-T_M$ case has therefore been forced to follow the same velocity profile as in $Coal_M$. The reduced residence time does increase the NO formation slightly but is not enough to cause the entire difference between $Coal_M$ and $Coal-T_M$. It therefore seems to be due to the lower temperature in the critical zone between 150 cm and 300 cm that causes the difference. Before that, the NO concentration is more or less the same, as well as the temperature. And after 300 cm, most of the fuel has been combusted and the formation of NO almost over.

It should be mentioned in relation to the discussion of the importance of volatile nitrogen release, that the simulation part of this work only considers gas phase chemistry. In reality, it is not only a question of when and where the nitrogen is released to the gas phase, but as mentioned previously also a question of how much is actually released with the volatiles or remains in the char. The partitioning of nitrogen and its heterogenous chemistry are important processes that are influenced by temperature-time history, (see for example Edland et al. [14]), but were not investigated as part of this work.

5. Conclusions

Torrefied and steam-exploded biomass have, independently, been co-combusted with Utah bituminous coal in a 1.5 MW_{th} combustion unit. By using sampling probes, temperature and gas composition have been determined for both co-combustion cases, as well as in a refence case with 100% bituminous coal. Replacing 15% of the bituminous coal with steam-exploded or torrefied biomass resulted in a reduction in NO concentration in the flue gas of 8% and 30%, respectively. These reductions are both larger than the 6% suggested by the lower nitrogen content in the biomass fuels compared to the coal. The torrefied wood pellets were also co-combusted in a 1.3 GW_{th} boiler, which also showed a clear reduction in NO larger than can be explained only by the lower nitrogen content in the fuel. The reason for this reduction was investigated by means of evaluating the experimental data and comparing it to detailed chemical reaction modeling. The model was shown to be capable of representing the combustion process and of capturing the trends also seen experimentally. It can be concluded that the type of pretreatment of a biomass has an influence on the formation of NO, even if the total nitrogen content remains the same. It is suggested that different pre-treatment methods will influence the release of volatile species and the nitrogen partitioning differently. Based on the presented results, it is shown that when and at what conditions the volatile nitrogen species are released plays a key role in the formation of NO. Knowing the properties of the mixed fuels, including PSD, nitrogen distribution and release pattern of different fuels, could in that way be used to manipulate the nitrogen chemistry to reduce NO emissions drastically when combining different fuels for co-combustion.

CRediT authorship contribution statement

Thomas Allgurén: Methodology, Software, Validation, Formal analysis, Investigation, Data curation, Writing – original draft, Visualization. **Klas Andersson:** Conceptualization, Methodology, Investigation, Writing – review & editing, Funding acquisition. **Andrew Fry:** Conceptualization, Investigation, Data curation, Writing – review & editing, Project administration, Funding acquisition. **Eric G. Eddings:** Conceptualization, Writing – review & editing, Project administration, Funding acquisition.

Declaration of Competing Interest

The authors declare that they have no known competing financial interests or personal relationships that could have appeared to influence the work reported in this paper.

References

[1] IPCC, Climate change 2021: The physical science basis, in: V. Masson-Delmotte, P. Zhai, A. Pirani, S.L. Connors, C. Péan, S. Berger, N. Caud, Y. Chen, L. Goldfarb, M.I. Gomis, M. Huang, K. Leitzell, E. Lonnoy, J.B.R. Matthews, T.K. Maycock, T. Waterfield, O. Yelekçi, R. Yu, B. Zhou (Eds.), Contribution of Working Group I to the Sixth Assessment Report of the Intergovernmental Panel on Climate Change, Cambridge University Press, Cambridge, 2021. In press.

[2] Z. Dobó, A. Fry, Investigation of co-milling Utah bituminous coal with prepared woody biomass materials in a Raymond Bowl Mill, Fuel 222 (2018) 343–349.

[3] X. Li, Y. Wang, T. Allgurén, K. Andersson, J.O.L. Wendt, The roles of added chlorine and sulfur on ash deposition mechanisms during solid fuel combustion, Proc. Combust. Inst. 38 (3) (2021) 4309–4316.

[4] T. Allgurén, J. Viljanen, X. Li, Y. Wang, K. Andersson, J.O.L. Wendt, Alkali sulfation during combustion of coal in a pilot scale facility using additives to alter the global sulfur to potassium and chlorine to potassium ratios, Proc. Combust. Inst. 38 (3) (2021) 4171–4178.

[5] K. Savolainen, Co-firing of biomass in coal-fired utility boilers, Appl. Energy 74 (3–4) (2003) 369–381.

[6] Y. Tu, J. Li, D. Chang, B. Hu, Effect of biomass co-firing position on combustion and NOX emission in a 300-MWe coal-fired tangential boiler, Asia Pac. J. Chem. Eng. 17 (1) (2022), e2734.

[7] C. Tang, W. Pan, J. Zhang, W. Wang, X. Sun, A comprehensive review on efficient utilization methods of High-alkali coals combustion in boilers, Fuel 316 (2022), 123269.

[8] L.S. Jensen, H.E. Jannerup, P. Glarborg, A. Jensen, K. Dam-Johansen, Experimental investigation of NO from pulverized char combustion, Proc. Combust. Inst. 28 (2) (2000) 2271–2278.

[9] A. Molina, E. Eddings, D. Pershing, A. Sarofim, Char nitrogen conversion: implications to emissions from coal-fired utility boilers, Prog. Energy Combust. Sci. 26 (4) (2000) 507–531.

[10] A. Molina, E.G. Eddings, D.W. Pershing, A.F. Sarofim, Nitric oxide destruction during coal and char oxidation under pulverized-coal combustion conditions, Combust. Flame 136 (3) (2004) 303–312.

[11] A. Molina, J.J. Murphy, F. Winter, B.S. Haynes, L.G. Blevins, C.R. Shaddix, Pathways for conversion of char nitrogen to nitric oxide during pulverized coal combustion, Combust. Flame 156 (3) (2009) 574–587.

[12] J.P. Spinti, D.W. Pershing, The fate of char-N at pulverized coal conditions, Combust. Flame 135 (3) (2003) 299–313.

[13] S.P. Visona, B.R. Stanmore, Modeling NOx release from a single coal particle II. Formation of NO from char-nitrogen, Combust. Flame 106 (3) (1996) 207–218.

[14] R. Edland, N. Smith, T. Allgurén, C. Fredriksson, F. Normann, D. Haycock, C. Johnson, J. Frandsen, T.H. Fletcher, K. Andersson, Evaluation of NOx-Reduction measures for Iron-Ore Rotary Kilns, Energy Fuel 34 (4) (2020) 4934–4948.

[15] J. Riaza, P. Mason, J.M. Jones, J. Gibbins, H. Chalmers, High temperature volatile yield and nitrogen partitioning during pyrolysis of coal and biomass fuels, Fuel 248 (2019) 215–220.

[16] J.H. Pohl, A.F. Sarofim, Devolatilization and oxidation of coal nitrogen, in: Symposium (International) on Combustion, Elsevier, 1977.

[17] D. Pershing, J. Wendt, Relative contributions of volatile nitrogen and char nitrogen to NOx emissions from pulverized coal flames, Industr. Eng. Chem. Proc. Design Dev. 18 (1) (1979) 60–67.

[18] D. Blair, J.O. Wendt, W. Bartok, Evolution of nitrogen and other species during controlled pyrolysis of coal, in: Symposium (International) on Combustion, Elsevier, 1977.

[19] X. Yang, Z. Luo, B. Yan, Y. Wang, C. Yu, Evaluation on nitrogen conversion during biomass torrefaction and its blend co-combustion with coal, Bioresour. Technol. 336 (2021), 125309.

[20] M.U. Alzueta, M. Borruey, A. Callejas, A. Millera, R. Bilbao, An experimental and modeling study of the oxidation of acetylene in a flow reactor, Combust. Flame 152 (3) (2008) 377–386.

[21] P. Glarborg, M.U. Alzueta, K. Dam-Johansen, J.A. Miller, Kinetic modeling of hydrocarbon/nitric oxide interactions in a flow reactor, Combust. Flame 115 (1–2) (1998) 1–27.

[22] P. Glarborg, M.U. Alzueta, K. Kjærgaard, K. Dam-Johansen, Oxidation of formaldehyde and its interaction with nitric oxide in a flow reactor, Combust. Flame 132 (4) (2003) 629–638.

[23] P. Glarborg, M. Østberg, M.U. Alzueta, K. Dam-Johansen, J.A. Miller, Twenty-Seventh Sysposium (International) on Combustion volume OneThe recombination of hydrogen atoms with nitric oxide at high temperatures, Symp. Combust. 27 (1) (1998) 219–226.

[24] P. Dagaut, P. Glarborg, M.U. Alzueta, The oxidation of hydrogen cyanide and related chemistry, Prog. Energy Combust. Sci. 34 (1) (2008) 1–46.

[25] J. Giménez-López, A. Millera, R. Bilbao, M.U. Alzueta, HCN oxidation in an O2/CO2 atmosphere: an experimental and kinetic modeling study, Combust. Flame 157 (2) (2010) 267–276.

[26] J. Giménez-López, M. Martínez, A. Millera, R. Bilbao, M.U. Alzueta, SO2 effects on CO oxidation in a CO2 atmosphere, characteristic of oxy-fuel conditions, Combust. Flame 158 (1) (2011) 48–56.

[27] M.U. Alzueta, R. Bilbao, P. Glarborg, Inhibition and sensitization of fuel oxidation by SO2, Combust. Flame 127 (4) (2001) 2234–2251.

[28] Y. Gao, P. Marshall, Kinetic studies of the reaction NH2 + H2S, Chem. Phys. Lett. 594 (2014) 30–33.

[29] P. Glarborg, Hidden interactions-Trace species governing combustion and emissions, Proc. Combust. Inst. 31 (I) (2007) 77–98.

[30] K.M. Thompson, Y. Gao, P. Marshall, Kinetic and theoretical investigations of the S + NO2 reaction, Int. J. Chem. Kinet. 44 (1) (2012) 90–99.

[31] T. Allgurén, Chemical interactions between potassium, nitrogen, sulfur and carbon monoxide in suspension-fired systems, in: Department of Space, Earth and Environment, 2017 Chalmers University of Technology, Göteborg, Sweden, 2017.

[32] T. Allgurén, K. Andersson, Influence of KCl and SO2 on NO Formation in C3H8 Flames, Energy Fuel 31 (10) (2017) 11413–11423.

[33] T. Ekvall, K. Andersson, T. Leffler, M. Berg, K–Cl–S chemistry in air and oxy-combustion atmospheres, Proc. Combust. Inst. 36 (3) (2017) 4011–4018.

[34] S. Hjärtstam, F. Normann, K. Andersson, F. Johnsson, Oxy-fuel combustion modeling: Performance of global reaction mechanisms, Ind. Eng. Chem. Res. 51 (31) (2012) 10327–10337.

[35] X. Wang, H. Tan, Y. Niu, M. Pourkashanian, L. Ma, E. Chen, Y. Liu, Z. Liu, T. Xu, Experimental investigation on biomass co-firing in a 300MW pulverized coal-fired utility furnace in China, Proc. Combust. Inst. 33 (2) (2011) 2725–2733.

[36] I. Rahimipetroudi, K. Rashid, J.B. Yang, S.K. Dong, Development of environment-friendly dual fuel pulverized coal-natural gas combustion technology for the co-firing power plant boiler: Experimental and numerical analysis, Energy 228 (2021), 120550.

[37] I. Rahimipetroudi, K. Rashid, J.B. Yang, S.K. Dong, Comprehensive study of the effect of a developed co-firing burner and its front-wall, opposed-wall, and tangential firing arrangements on the performance improvement and emissions reduction of coal-natural gas combustion in a boiler, Int. J. Therm. Sci. 173 (2022), 107379.

[38] C.A. Wang, C. Wang, X. Jia, L. Zhao, P. Wang, D. Che, NO formation characteristics and fuel-nitrogen transformation mechanism during co-firing of low-volatile carbon-based solid fuels with bituminous coal, Fuel 291 (2021), 120134.